RJC
http://www.rasayanjournal.com

RASĀYAN *J. Chem.*
Vol.3, No.4 (2010), 783-795
ISSN: 0974-1496
CODEN: RJCABP

INHIBITORY EFFICACY OF *PIPER NIGRUM LINN.* EXTRACT ON CORROSION OF AA1100 IN HCL

Rekha N. Nair, Shashi Sharma, I. K. Sharma, P. S. Verma, Alka Sharma*
Department of Chemistry, University of Rajasthan, Jaipur (Rajasthan) INDIA
*E-mail: sharma_alka21@yahoo.com

ABSTRACT

The inhibitory propensity of the *Piper nigrum Linn.* seeds for acid corrosion of aluminium alloy (AA1100) was investigated employing weight loss method. Kinetic and adsorption parameters were calculated. The inhibition efficiency was found to increase with increase in inhibitor concentration. The experimental data were fit in to the El-Awady's thermodynamic–kinetic model. Surface analysis was carried out by FT-IR to ascertain the anti-corrosive property of the inhibitor.

Keywords: *Aluminium; Weight loss; FT-IR spectroscopy; Acid inhibition; Kinetic and Adsorption parameters*

INTRODUCTION

Use of inhibitors is one of the most practical methods for protection against corrosion especially in acid solutions to prevent metal dissolution and acid consumption. Corrosion inhibitors reduce or prevent the reactions taking place at anode or cathode. They are adsorbed on metal surface and form a barrier to oxygen and moisture by complexing with metal ions or by removing corrodent from the environment. Some of the inhibitors facilitate formation of passivating film on the metal surface[1-5]. Although synthetic chemicals are the most effective corrosion inhibitors but they are highly costly, toxic and threat to the environment. They may cause reversible (temporary) or irreversible (permanent) damage to organ system. The toxicity may manifest either during the synthesis of the compound or during its applications. The safety and environmental issues of corrosion inhibitors arisen in industries has always been a global concern. Hence, it is necessary to find out corrosion prevention by low cost, easily available and environmentally acceptable i.e. eco-friendly (*green*) inhibitors.

The natural products are easily available and also biodegradable in nature, hence safe to the environment. Their extracts contain a large variety of organic compounds with which they get adsorbed on the metal surface by displacing water/solvent molecules and form a compact barrier film and hence combating metal dissolution to a considerable extent[6-16]. Combating metal corrosion by "*eco-friendly* (*green) inhibitors*" shows environmental awareness and concern besides cost efficacy and energy conservation. In view of that, an attempt has been made to investigate the inhibitory propensity of *Piper nigrum L.* seeds on acid corrosion of aluminium alloy.

Literature survey reveals that *Piper nigrum L.* seeds contain 5-9 % of the alkaloids Piperine, Piperidine, Piperittine, and 1-2.5 % of volatile oil, the major constituents of which are α- and β-pinene, limonene and phellandrene[17-19]. In one study, the black pepper (Piperaceae) was found to comprise 33.7 % β-caryophyllene, besides, Chavicine, Thiamine, Riboflavin, Nicotinic acid, resins and metals like Ca, P, and Fe [20]. Most among these organic compounds are antibacterial, fungicide, and antioxidants, moreover, the compounds like piperine, piperidine, thiamin, riboflavin, nicotinic acid, etc. possess nitrogen and oxygen which strengthen their adsorptive property over metal surface and hence the anti-corrosive behaviour[21-25].

The ethanolic extract of *Piper nigrum L.* seeds (EE*PnL*S) was used to evaluate its anti-corrosive property on corrosion of aluminium alloy (AA1100) in 0.5 M HCl by chemical method. The adsorption behaviour of EE*PnL*S on the surface of AA1100 was justified by FT-IR spectroscopy. The inhibitory action of EE*PnL*S was satisfactorily explained and various adsorption isotherms were tested to fit in to the results. On the basis of the results, it is suggested that EE*PnL*S can be used as *green inhibitor* for acid corrosion

of aluminium and can replace conventional inorganic/organic inhibitors which are expensive and also toxic to living beings.

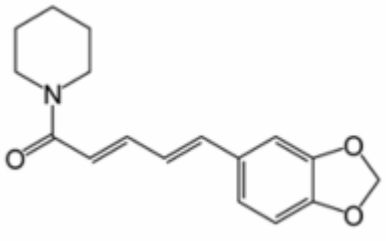

Piperine

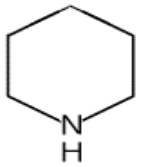

Piperidine

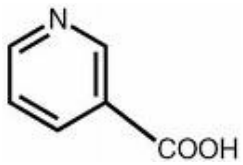

Niacin (Nicotinic acid)

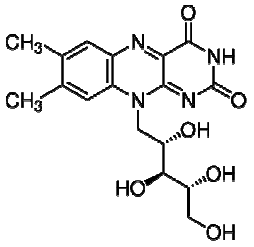

Riboflavin

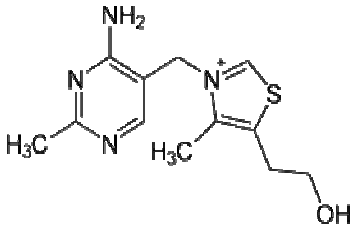

Thiamine

EXPERIMENTAL

Chemical Method (Weight Loss Measurements)

The progress of the corrosion was monitored by determining the weight loss of the coupons at a fixed time intervals. All the experiments were performed at 30 ± 1 ^{0}C and in duplicate to check the reproducibility of the results. Average values of weight loss were reported. All the chemicals, acids and reagents used were of analytical grade. Bidistilled water was used for the preparation of solutions.

Test coupons

The industrially used Aluminium (AA1100) of 99 % purity (Fe-0.95%; Mn-0.05%; Cu-0.05-0.20%; Zn-0.10%; rest aluminium) having dimensions 3 cm x 2 cm x 0.15 cm with a hole of about 0.12mm diameter near the upper edge for the purpose of hanging were used as test coupons. Before each experiment, the coupons were examined carefully to check for rough edges and the surface treatment of the coupons was done by polishing with emery papers and washed with distilled water and finally with acetone and then dried in oven at 60^0 C for about half an hour. They were then kept in desiccators until cooled to room temperature and then weighed accurately using a digital balance (Adair Dutt 205 A ACS). They were subjected to further heating, cooling and weighing till a constant weight was obtained and was stored in desiccators before use. Each coupon was suspended by a glass hook and immersed in a covered beaker containing 100 ml of the unstirred test solution at room temperature for a defined period of time. Later, the test coupons were cleaned with distilled water and then dried in an oven for 20 minutes and finally they were weighed to evaluate weight loss.

Test media

The electrolyte solution was prepared by dilution of analytical grade 36 % HCl with bidistilled water and thereafter its standardization.

Ethanolic Extract of *Piper Nigrum L.* Seeds (EE*PnL*S)

The stock solution of *Piper nigrum L.* seeds extract was prepared by soaking room temperature-dried and finely powdered seeds in a properly corked container containing distilled ethanol. On completion of soaking period, the ethanolic solution was refluxed, thereafter, distilled to concentrate the inhibiting chemicals and finally filtered to remove any suspended impurities. The mass of plant extract was dried and evaluated as 9.15 g/L.

Test Solutions

The corrosive solution (100 ml of 0.5 M HCl) was measured into six separate beakers (250 ml) numbering S-0, S-1, S-2, S-3, S-4 and S-5. EE*PnL*S was added in these beakers (S-1 to S-5) in the order of increasing concentrations so as to have 0.0915, 0.1830, 0.2745, 0.3660 and 0.4575 g/L respectively. No extract was added to the first beaker (S-0). All the beakers were covered with Teflon tape and kept unstirred throughout the experiment.

The corrosion behaviour of coupons (AA1100) was investigated for various immersion periods (72 to 288 h) in 0.5 M HCl, in absence and presence of EE*PnL*S, at room temperature (~30 ± 1 ^{0}C). For each experiment, after fixed period of immersion, the cleaning, drying and weighing of the test coupons was done to evaluate weight loss. The effect of variation of EE*PnL*S concentration was also carried out and thereafter, the optimum concentration for effective inhibitory action of EE*PnL*S was evaluated.

Surface Analysis (FTIR Spectroscopy)

The adsorbed film of EE*PnL*S on the surface of the coupon was analyzed using FT-IR (KBr pellet method) spectroscopy. FT-IR was conducted on 8400 S Shimadzu, Japan FT-IR spectrometer in the IR range from 4000 to 400 cm^{-1}. The spectras of the vacuum dried EE*PnL*S and the surface-adsorbed EE*PnL*S were compared for elucidation of its adsorption behaviour on metal surface. The adsorptive tendency was obvious from these IR spectra.

RESULTS AND DISCUSSION

Corrosion Behaviour of AA1100 in 0.2 M and 0.5 M HCl

The corrosion behaviour of AA1100 in corrosive media alone (i.e. 0.2 M and 0.5 M HCl) at room temperature was illustrated in Fig.1. It clearly illustrate that the weight loss of AA1100 coupons increases with increasing acid strength. This is due to fact that the rate of chemical reaction increases with increasing acid concentration and / or probably due to increase in the rate of diffusion and ionization of active species in the corrosion reaction.

Thus, the inhibitive action of EE*PnL*S on corrosion of AA1100 was investigated in 0.5 M HCl. The experimental data so obtained using different concentrations of EE*PnL*S for various immersion time periods at 30 ± 1 ^{0}C were analyzed and put forward.

Effect of Varying Immersion Time and Concentrations of EE*PnL*S

The effect of increasing immersion time and concentrations of EE*PnL*S on the weight loss of AA1100 coupons in uninhibited and inhibited conditions was illustrated in Fig. 2. The weight loss was found to increase with immersion period in corrosive as well as inhibited solutions. The increase in weight loss values with exposure time is an indication of continuous active corrosion reactions. On adding EE*PnL*S to the aggressive solution, it fell appreciably below than that of the aggressive solution alone, depicting inhibitory propensity of EE*PnL*S.

Similarly, with increasing concentration of EE*PnL*S a comparable decrease in corrosion rate of AA1100 and hence an increase in protective efficiency of EE*PnL*S as a function of its concentration was observed (Figs. 3 and 4). The maximum IE (85.69 %) with corresponding minimum corrosion rate (ρ_{corr} = 0.4906 mmpy) was observed at the higher concentration (0.4575 g/L) of EE*PnL*S on corrosion of AA1100 in 0.5 M HCl at 72 h exposure time at 30 ± 1 ^{0}C (Table-1).

From the experimental data, the corrosion parameters, i.e. corrosion rate (ρ_{corr}) (mmpy), percentage inhibition efficiency (IE %), fractional surface coverage (θ), adsorption equilibrium constant (K_{ad}) etc. were evaluated and tabulated in Table-1.

The corrosion rate (ρ_{corr}) with respect to exposure time was found to decrease sharply at lower concentrations of EE*PnL*S, but at higher concentrations of EE*PnL*S it was observed to increase, though very slightly. As a result of which, the overall corrosion rate was found to reach a static value (≅1.3 mmpy) at higher exposure time period (288 h) (Table-1 and Fig. 3). Thus clearly indicating that at higher exposure time period the corrosion rate was observed to be independent of concentration of EE*PnL*S. The

same trend was observed for IE (%) i.e. with increase in immersion time a comparable decrease in the IE (%) of EE*PnL*S (Fig. 4).

From Table-1 and Fig. 4, it is clear that the effective inhibitory action of EE*PnL*S was observed at its higher concentration (0.4574 g/L) for all exposure times, indicating its optimum concentration on acid corrosion of AA1100 in 0.5 M HCl at 30 ± 1 ^{0}C. The increase in IE (%) of EE*PnL*S with its concentration (Fig. 4), at 72 h exposure time, may be attributed to the more surface area covered by the adsorbed molecules of EE*PnL*S with an increase in its concentration, thereby decreasing the available reaction area (geometric blocking effect) on the AA1100 surface[26]. The active ingredients (such as, alkaloids Piperine, Piperidine, Piperittine, Thiamine, Riboflavin, Nicotinic acid, resins, etc.) present in black pepper[17-20], gets easily adsorbed on the corroding metal giving rise to high protective efficiency. The high inhibition efficiency may also be due to the synergistic action of all these organic constituents present in the EE*PnL*S, as these compounds contains nitrogen and oxygen which may enhances its adsorptive property over AA1100 surface[20-25].

Kinetic Analysis of Weight Loss Results

The mechanism of corrosion inhibition for an inhibitor can be explained by a kinetic-thermodynamic model. Assuming the corrosion rate of aluminium against the concentration of EE*PnL*S obeys the kinetic relationship [27-28]:

$$\log \rho_{corr} = \log k + B \log C \quad (1)$$

where, k is the rate constant and equals to ρ_{corr} at inhibitor concentration of unity; B is the reaction constant which in the present case is a measure for the inhibitor effectiveness and C is the concentration of EE*PnL*S in g/L.

Fig.5 clearly illustrates a linear relationship between log ρ_{corr} vs. log C at 30 ± 1 ^{0}C for 0.5 M HCl, which confirm that the kinetic parameters (k and B) can be calculated by using the above equation. Besides, the negative slopes of the lines depict that the rate of corrosion process is inversely proportional to EE*PnL*S concentration, i.e. EE*PnL*S becomes more effective with increasing its concentration.

Corrosion reaction is an overall reaction in which both solid and liquid phases are consumed. It is therefore difficult to apply most of the principles of the chemical kinetics to corrosion reaction. A plot of the log of the measured weight of the AA1100 coupons after post treatment (log W_f) against time (t) helps to explain the kinetics of the corrosion of AA1100 in 0.5 M HCl in the corrodent and corrodent-inhibitor system (Fig. 6), clearly depicting a linear variation, thus further confirming a first order kinetics formulated [26-27] as:

$$\log W_f = \log W_o - Kt \quad (2)$$

where, W_f and W_o are weights post treatment of coupons and initial weight before immersion respectively; K is the rate constant for corrosion process; and t is the inversion time (h).

Adsorption Isotherms

The primary step in action of inhibitors in acid solution is adsorption on to the metal surface. The adsorption of an inhibitor species, Inh., on metal surface in aqueous solutions should be considered as a substitution reaction and the process can be expressed as [28]:

$$Inh._{sol} + x\, H_2O_{ads} \Leftrightarrow Inh._{ads} + x\, H_2O_{sol} \quad (3)$$

where x, the size ratio, is the number of water molecules displaced by one molecule of inhibitor during adsorption process. In this process Bockris *et. al*[29] have assumed that water molecules dipoles have to be oriented and their orientation depends on the metal charge adapting the suitable adsorption isotherm.

Adsorption isotherm provides useful insights into the mechanism of corrosion inhibition. The adsorption equilibrium constant, K_{ad}, is expressed as:

$$K_{ad}\, C = \theta / (1 - \theta) \quad (4)$$

where C is the concentration of EE*PnLS* in g/L; θ the fractional surface coverage and K_{ad} is the adsorption equilibrium constant. The fractional surface coverage, θ, was evaluated [30] and tabulated in Table-1. The fractional surface coverage, θ, and the adsorption equilibrium constant, K_{ad}, was found large at higher concentration of EE*PnLS*, hence it is understood that higher concentration of EE*PnLS* is essential for maximum adsorption over AA1100 surface.

It is necessary to determine empirically which adsorption isotherm fits best to the surface coverage data in order to use the corrosion rate measurements to calculate the thermodynamic parameters pertaining to inhibitor adsorption. The Langmuir isotherm was tested for its fit to the experimental data. Langmuir isotherm expressed as: $\log (\theta / 1-\theta) = \log K_{ad} + \log C$, is based on the assumption that all adsorption sites are equivalent and that particle binding occurs independently from nearby sites being occupied or not and also that the adsorbed molecule decreases the surface area available for the corrosion reactions to occur[26-28]. Though the plot (Fig. 7) of $\log (\theta / 1-\theta)$ vs. log C was linear, the deviation of the slopes from unity (for ideal Langmuir isotherm) can be attributed to the molecular interaction among the adsorbed inhibitor species, a fact which was ignored during the derivation of the Langmuir isotherm equation.

Hence to explain the nature of the adsorption of EE*PnLS* on AA1100 surface, the experimental data were fit in to the El Awady's thermodynamic-kinetic model[27-31], which is expressed as: $\log (\theta / 1-\theta) = \log K_{ad} + y \log C$; where, θ is the degree of surface coverage, C is the inhibitor concentration in the bulk of solution, K_{ad} is the binding constant of the adsorption reaction and $K_{ad}^{(1/y)} = K$, equilibrium constant, 1/y is the number of inhibitor molecules occupying one active site (or number of the water molecules replaced by one molecule of inhibitor). Curve-fitting of the data according to the thermodynamic-kinetic model at 30 ± 1 ^{0}C illustrated the linear dependence of $\log \theta / (1-\theta)$ as a function of log C (Fig. 7).

The K_{ad} is related to the free energy of adsorption ΔG^0 as:

$$K_{ad} = (1 / C_{solvent}) \exp^{(-\Delta G / RT)} \quad (5)$$

where $C_{solvent}$ represents the molar concentration of the solvent (in case of water it is 55.5 mol/dm^3); R = universal gas constant; and T = temperature (K). Using above expression the free energy of adsorption, (ΔG^0) (in kJ/mol), was evaluated for corrodent-EE*PnLS* system for optimum concentration of EE*PnLS* (0.4575g/L) at 72 h exposure time and 303 ± 1 K. The ΔG^0 value was observed as –16.59 kJ/mol. This clearly indicates that the adsorption of the active species of EE*PnLS* over the surface of AA1100 in 0.5 M HCl was of physical nature. The negative values of ΔG^0 ensure the spontaneity of the adsorption process and stability of the adsorbed layer on the metal surface. Generally, ΔG^0 upto –20 kJ/mol are consistent with the electrostatic interactions between the charged molecules and the charged metal showing physisorption of EE*PnLS* over AA1100 surface, whereas, $\Delta G^0 \geq -40$ kJ/mol are associated with chemisorption because of sharing or transfer of electrons from the inhibitor molecules to the metal surface to form a coordinate type of bond[26-27]. The values of thermodynamic functions are very approximate because the inhibition efficiency is dependent on time, as is the surface coverage (θ).

Surface Analysis:

FT-IR Spectroscopy

The adsorption of EE*PnLS* on AA1100 was further confirmed by comparing the IR spectra of vacuum dried EE*PnLS* with the spectra of its adsorbed film over AA1100 surface in 0.5 M HCl at exposure time period of 72 h (Figs. 8 and 9). Identification of various functional groups present in the EE*PnLS* is needed to understand the adsorption mechanism.

Fig. 8 is the FT-IR spectrum of EE*PnLS* which clearly shows the presence of hydroxyl group in EE*PnLS* by the broad and strong peaks in the region 3600 to 3200 cm^{-1} which are assigned to overlapping of –OH, consistent with the peak at 1100 cm^{-1}due to alcoholic C–O stretching vibration[32-34]. The N–H stretching vibrations are also distinct in region from 3550 to 3300 cm^{-1} and at 1640 cm^{-1}. The strong bands at 1290, 2850, 2900 cm^{-1} and a weak band at 3070 cm^{-1} may be ascribed to aliphatic and aromatic C–H stretching respectively. The peaks at 1700–1615 cm^{-1} are due to C=N stretching (similar conjugate effects to C=O). The peak at 1730 cm^{-1} can be assigned to a C=O stretching in aldehydic and acidic; and at 1625–1500

cm^{-1} in the carboxylate (salts) as well as amino acid zwitter ions. These are also consistent with the bands in the regions 2800–2750 cm^{-1} and 3500–2600 cm^{-1} assigned to aldehydic C–H and acidic O–H stretching vibrations respectively. The absorption band occurring at 1685 cm^{-1} goes for C=O stretching due to aromatic ketones. Absorptive peaks in the range of 1300–1240 cm^{-1} can be assigned to a C–O stretching in carboxyl groups as well as the C–N stretching vibrations in aromatic amines. Thus the EE*PnL*S contains mixtures of organic compounds.

In the FT-IR of coupon-scratched EE*PnL*S (Fig. 9), certain peaks were found disappeared completely and some shifted to higher frequency region, proving that some adsorption has been taking place over the AA1100 surface (Fig. 9). The significant changes in the FT-IR spectrum may be noted at wave numbers of 3200–3600 and 1640; 2830–2900; 1730; 1700–1615; 1685; 1300–1220; 1260–1220; 1100 cm^{-1} which are assigned to O–H (well broad) as well as N–H; C–H (variable); C=O (aldehyde/acidic); aromatic ketonic; N–H, C=N and C–O (alcohol/ethers) stretchings respectively. As aluminium is unlikely to be attached to a carbon atom, these changes suggest the possibility that the electronegative hetero atoms of EE*PnL*S (such as –N and –O) are involved in this adsorption process as well. Thus, the surface analysis using FT-IR reveals that functional groups like –OH, –COOH, N–H, C=N, C=O, C–O present in the organic constituents of EE*PnL*S are involved in adsorption on AA1100 via hydrogen bonding and/or weak van der Waals forces.

Proposed Mechanism for Inhibition by EE*PnL*S

The mechanism of inhibition can be understood by knowing the mode of interaction of the inhibitor molecules with the electrode. Inhibitors function by adsorption and/ or hydrogen bonding to the metal[35]. This in turn depends on the chemical composition and structure of the inhibitor, the nature of the metal surface, and the properties of the medium. Structural and electronic parameters, such as the type of functional group, steric and electronic effects, are generally responsible for the inhibition efficiency of any inhibitor, that is, the adsorption mechanism. Since the compound has to block the active corrosion sites present on the metal surface, the adsorption occurs by the inhibitor's free electrons linking with the metal. The plant extracts constitutes organic compounds [6-9, 11-25, 28] containing:

1. Lone pair of electrons present on a hetero-atom (eg. N, S, P, O);
2. π- bond, (these molecules are the most effective but often harmful to the environment);
3. Triple bond (eg. cyano groups); and
4. Heterocyclic compounds such as pyridine ring pyrrole, imidazole, etc.

The black pepper seeds comprise alkaloids piperine, piperidine, piperittine, volatile oil (the major constituents of which are α- and β-pinene, limonene and phellandrene), β-caryophyllene, Chavicine, Thiamine, Riboflavin, Nicotinic acid, resins, aromatic oils and metals like Ca, P, and Fe[17-20]. Most among these organic compounds possess hetero atoms such as O– and N– which strengthen their adsorptive property over metal surface and hence the anti-corrosive behaviour[21-25].

As a rule of thumb it holds that N–containing compounds exert their best efficiencies in HCl [28], thus, it can be suggested that the high IE (%) of EE*PnL*S may be due to the active organic constituent of EE*PnL*S containing O– and N–. The inhibiting influence of these molecules is attributed to their adsorption through the –NH, C=O, OH, COOH etc. groups and also may be due to the presence of more π-electrons in the rings[23]. It is also suggested that they may act together (synergistically) for their better protective performance towards acid corrosion of aluminium. These organic molecules get physisorbed on the metal surface forming a protective film. In the present case, EE*PnL*S consisted of O– and N– containing groups which orient themselves over the metal surface so as to cover it horizontally via weak bonding. The adsorbed organic molecules may interact with each other as well as with the electrode surface. In the process water molecules must be displaced from the metal surface. The possible mode of adsorption of these compounds on the AA1100 surface is depicted below (Fig. 10):

CONCLUSIONS

- The analyses indicate that the in acid medium EE*PnLS* inhibited metal dissolution to a large degree (IE = 85.69 % at 30 ± 1 ^{0}C).
- The adsorption mechanism of EE*PnLS* on AA1100 surface was well expressed by the El-Awady's Thermodynamic-kinetic model.
- The nature of the adsorption of EE*PnLS* on metal surface was evaluated as physisorption.
- FTIR spectra further confirm the formation of the protective film.
- The results obtained from chemical (weight loss) and surface analysis methods reinforce the anti-corrosive property of EE*PnLS* for acid corrosion of AA1100.
- The EE*PnLS* can act as a good inhibitor for combating corrosion of AA1100 in HCl.
- *Piper nigrum L.* seeds extract, an eco-friendly corrosion inhibitor, thus, has potential to be a good replacement for many toxic chemicals used as corrosion inhibitor of Aluminium and its alloys in HCl medium

ACKNOWLEDGEMENTS

Authors are highly thankful to Prof. Renuka Jain, Head, Department of Chemistry, University of Rajasthan, Jaipur for providing necessary research facilities. Rekha N. Nair thanks to Dr. S. M. Seth, Chairman, Mr. Shashi Kant Singhi, Director, Poornima College of Engineering, Jaipur for their kind support and encouragement.

REFERENCES

1. S. Divakara shetty, Prakash Shetty, and H. V. Sudhaker Nayak, *J. Chil. Chem. Soc.,* **51(2)**,849(2006)
2. T. Sethi, A. Chaturvedi, R. K. Upadhyay and S. P. Mathur, *J. Chil. Chem. Soc*., **52** (3),1206(2007)
3. T. Sethi, A. Chaturvedi, R. K. Upadhyay and S. P. Mathur, *J. Chil. Chem. Soc.,* **52 (3)**,1206(2007)
4. Anees A. Khadom, Aprael S. Yaro, Abdul Amir H. Kadhum, *J. Corros. Sci. Engg.,* **12(18)** ,1466(2009)
5. Zarrouk, T. Chelfi , A. Dafali , B. Hammouti , S.S. Al-Deyab, I. Warad, N. Benchat, M. Zertoubi , *Int. J. Electrochem. Sci.,* **5** ,696 (2010).
6. Rekha N. Nair, Nemichand Kharia, I. K. Sharma, P. S. Verma, Alka Sharma, *J. Electrochem. Soc. India,* **56 (1/2)** ,41(2007).
7. S. A. Umoren, I. B. Obot, E. E. Ebenso, *E-J. Chem.,* **5 (2)** ,355(2008).
8. A.M. Abdel-Gaber, B.A. Abd-El-Nabey, I.M. Sidahmed, A.M. El-Zayady, M. Saadawy, *Mater. Lett.,* **62 (1)** ,113(2008).
9. Pandian Bothi Raja, Mathur Gopalakrishnan Sethuraman, *Mater. Lett.,* **62 (1)** ,113(2008).
10. S. Rajendran, J. Jeyasundari, P. Usha, J. A. Selvi,B. Narayanasamy, A. P. P. Regis, P. Rengan, *Portug. Electrochimica Acta,* **27 (2)** ,153(2009).
11. F.S. de Souza, A. Spinell, *Corros. Sci.,* **51 (3)** ,642(2009).
12. A.M. Abdel-Gaber, B.A. Abd-El-Nabey, M. Saadawy, *Corros. Sci.,* **51 (5)** ,1038(2009).
13. A. O. James and O. Akaranta, *Afric. J. Pure Appl.Chem.*, **3 (12)** ,262(2009).
14. N. O. Eddy, P. A. P. Mamza, *Port. Electrochim. Act.,* **27 (4)** ,443(2009).
15. O. Ouachikh, A. Bouyanzer, M. Bouklah, J. M. Desjobert, J. Costa, B. Hammouti, L. Majidi, *Surf. Rev. Lett*., **16 (1) ,**49(2009).
16. Alka Sharma, P. S. Verma, I. K. Sharma, Rekha N. Nair, *Proc. World Acad. Sci. Eng. Technol. (PWASET)* **39 ,**745(2009).
17. Ernst Spath, Georg Englaender, Berichte der Deutschen Chemischen Gesellschaft [Abteilung] B: Abhandlungen, **68 B** ,2218(1935).
18. W. C. Evans, *Trease and Evans' Pharmacognosy*, WB Saunders Company Ltd.: London (1996).

19. G. Samuelsson, *Drugs of Natural Origin: a Textbook of Pharmacognosy,* Swedish Pharmaceutical Press: Stockholm (1999).
20. S. Tewtrakul, *et. al*, *J. Essential Oil Res.,* **12** ,603(2000).
21. Gurdip Singh, P. Marimuthu, C. Catalan, M. P. deLampasona, *J. Sci. Food Agri.*, **84 (14)** ,1878(2004)
22. S. Muralidharan, R. Chandrasekar, S. V. K. Iyer, *Proc. Ind. Acad. Sci. (Chem. Sci.)*, **112 (2)** 127(2000)
23. K.F. Khaled, K. Babic´-Samardzija, N. Hackerman, *J. Appl. Electrochem.,* **34** ,697(2004).
24. S. Malhotra, *Ph. D. Thesis*, Chemistry Department, University of Delhi, Delhi (2005).
25. Pandian Bothi Raja, Mathur Gopalakrishnan Sethuraman, *Mater. Lett.,* **62 (17-18)** ,2977(2008).
26. P. W. Atkins, *Chemisorbed and Physisorbed Species, A Textbook of Physical Chemistry,* University Press Oxford: NY 936(1980).
27. P. W. Atkins, J. de Paula, *Physical Chemistry,* Oxford University Press: NY (2002).
28. Ehteram A. Noor*, Int. J. Electrochem. Sci.,* **2 ,**996 (2007).
29. J. O' M. Bockris, A. K. N. Reddy, *Modern Electrochemistry - Electrodics in Chemistry, Engineering, Biology, and Environmental Science*, 2nd ed., Kluwer Academic / Plenum Publishers: New York, 2B (2000).
30. B. B. Damaskin, *Adsorption of Organic Compounds on Electrodes*, Plenum Press: New York 221(1971).
31. S. A. Umoren, E. E. Ebenso, *Mater. Chem. Phys.*, **106** ,387(2007).
32. R.L. Shriner, C.K.F. Hermann, T.C. Morrill, D.Y. Curtin, R.C. Fuson, *The Systematic Identification of Organic Compounds*, 7th ed., Wiley: New York (1998).
33. R. M. Silverstein, G. C. Bassler, T. C. Morrill, *Spectroscopic Identification of Organic Compounds,* John Wiley & Sons: New York (1981).
34. P. S. Kalsi, *Spectroscopy of Organic Compounds,* 6th ed., New Age International (Pvt.) Ltd. Publishers: New Delhi (2004) (reprint 2008).
35. K. Aramaki and N. Hackerman, *J. Electrochem. Soc.,* **115** ,1007(1968).

[RJC-693/2010]

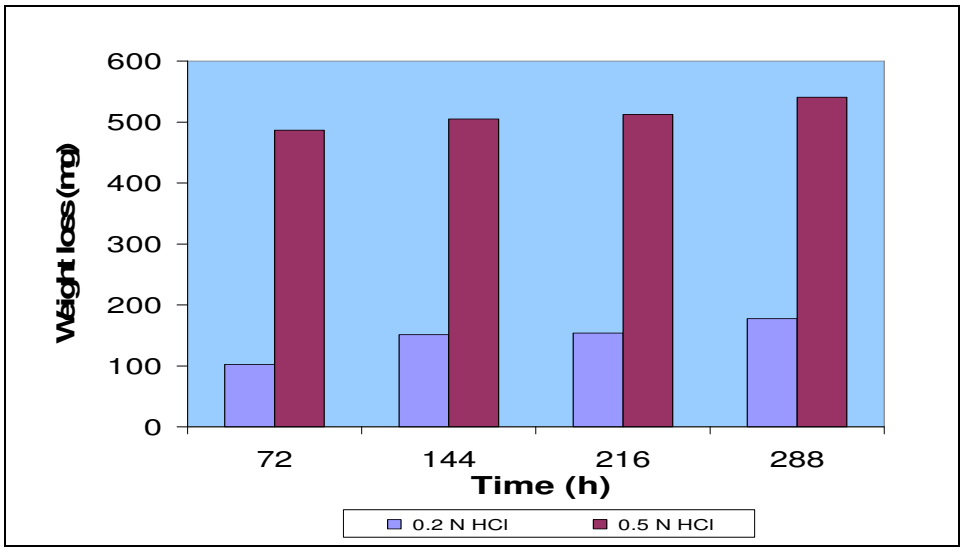

Fig.-1: Weight Loss vs. Immersion Time for AA1100 coupons in 0.2 M and 0.5 M HCl at 30 ± 1 ^{0}C.

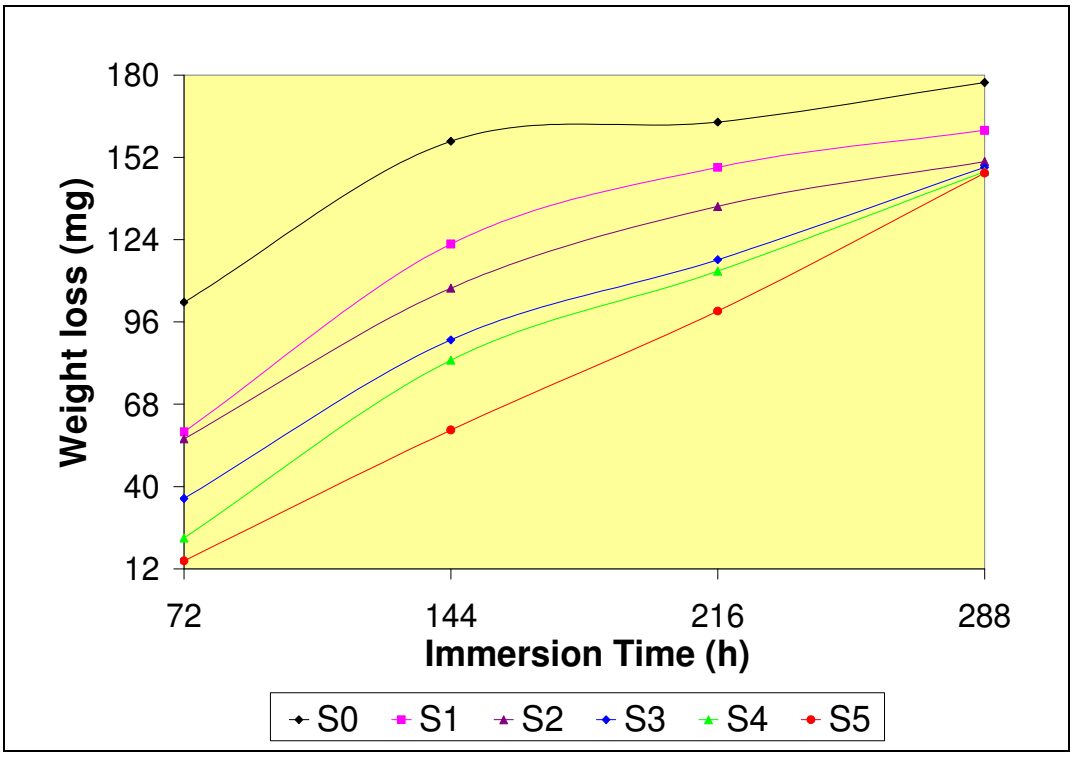

Fig.-2: Weight loss (mg) vs. Immersion Time (h) for AA1100 coupons with different concentrations of EE*PnLS*.

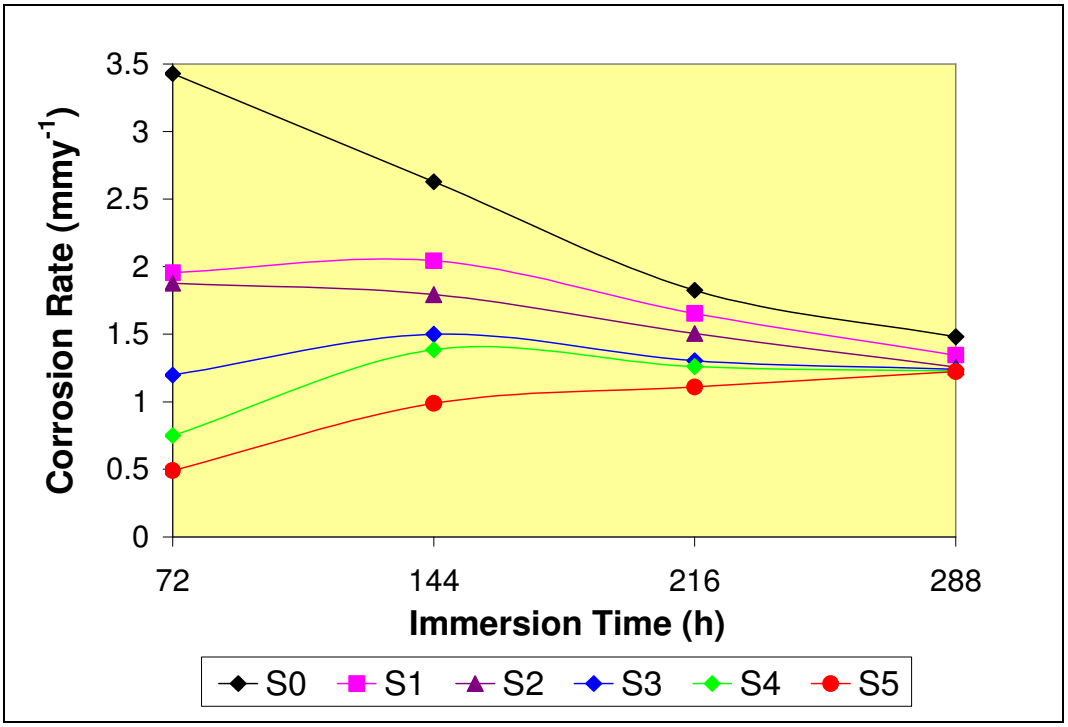

Fig.-3: Corrosion Rate (ρ_{corr}) (mmy^{-1}) vs. Immersion Time (h) for AA1100 coupons with different concentrations of EE*PnLS*.

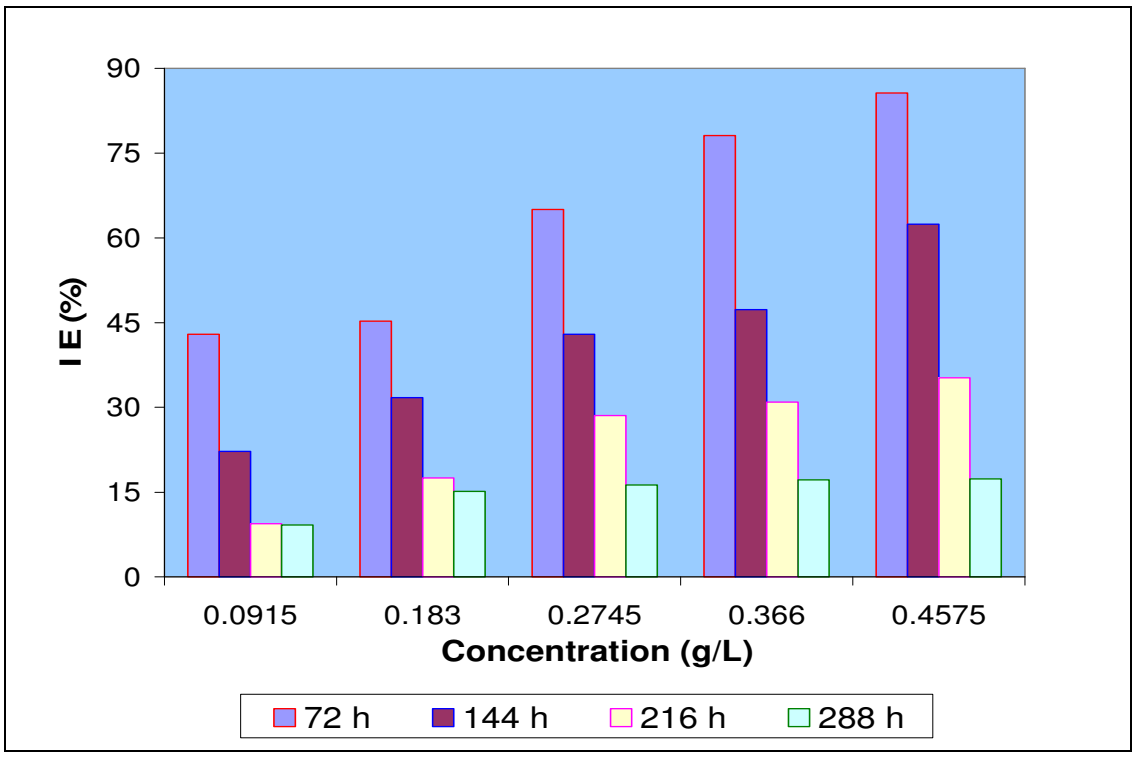

Fig.-4: Inhibition Efficiency (%) vs. EE*PnLS* Concentration (g/L) at various Immersion Time (h).

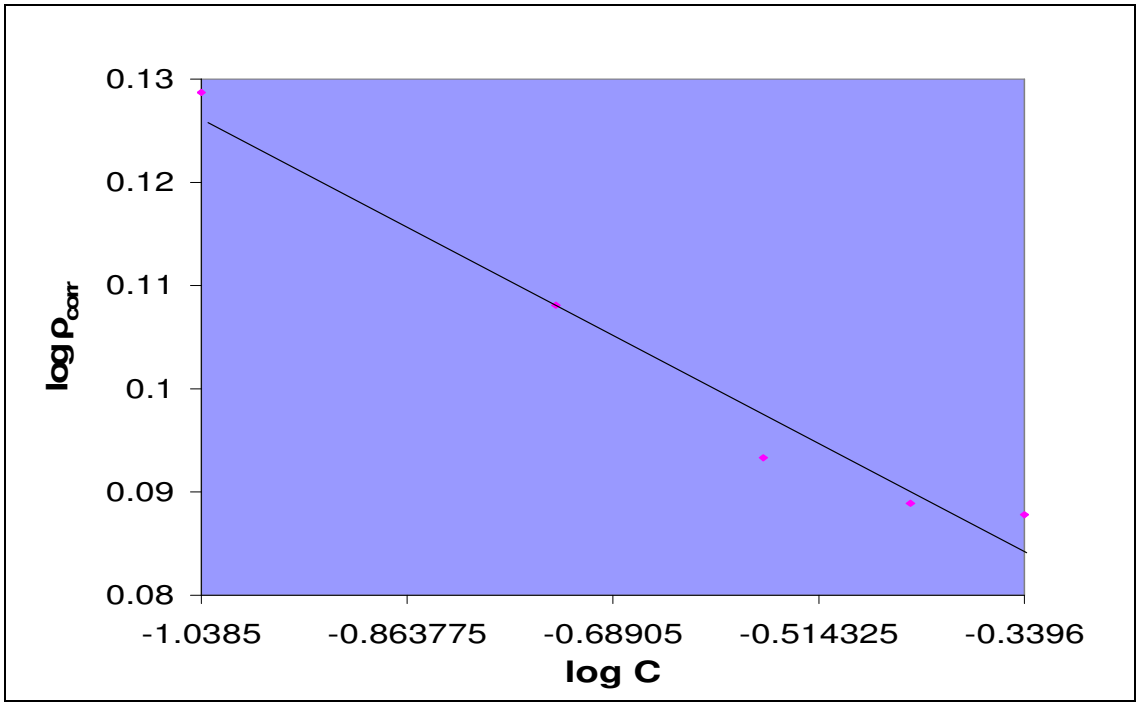

Fig.-5: log ρ_{corr} vs. log C.

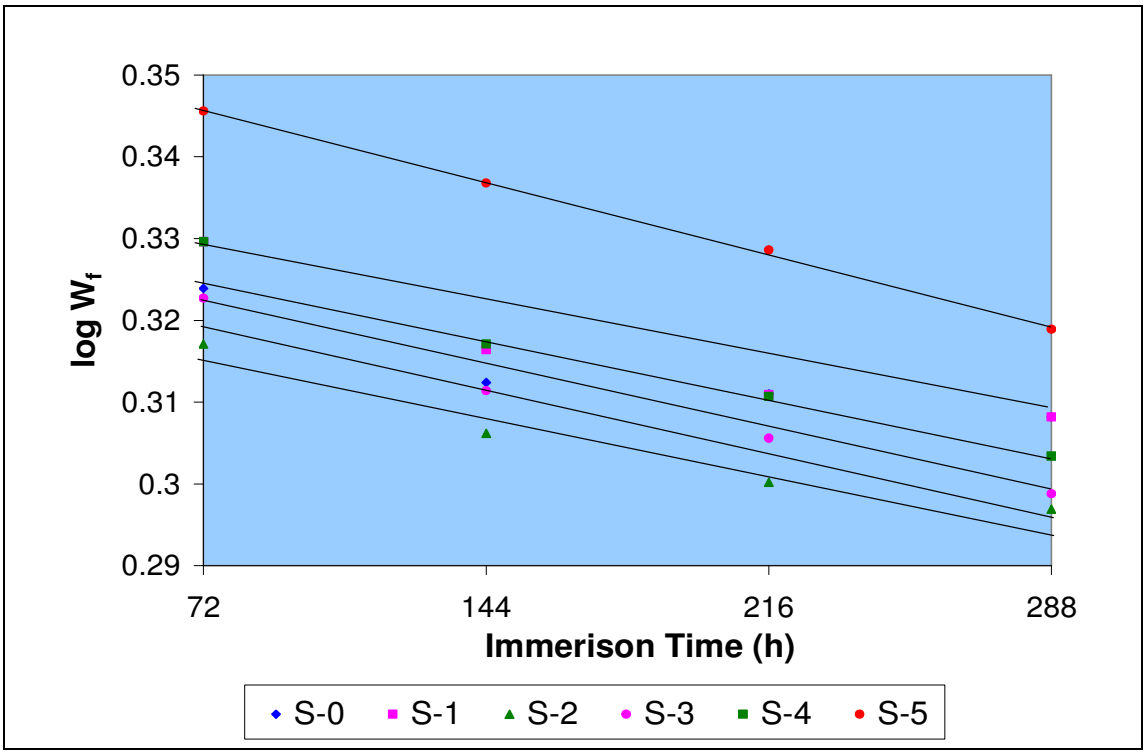

Fig.-6: log W_f vs. Immersion Time (h)

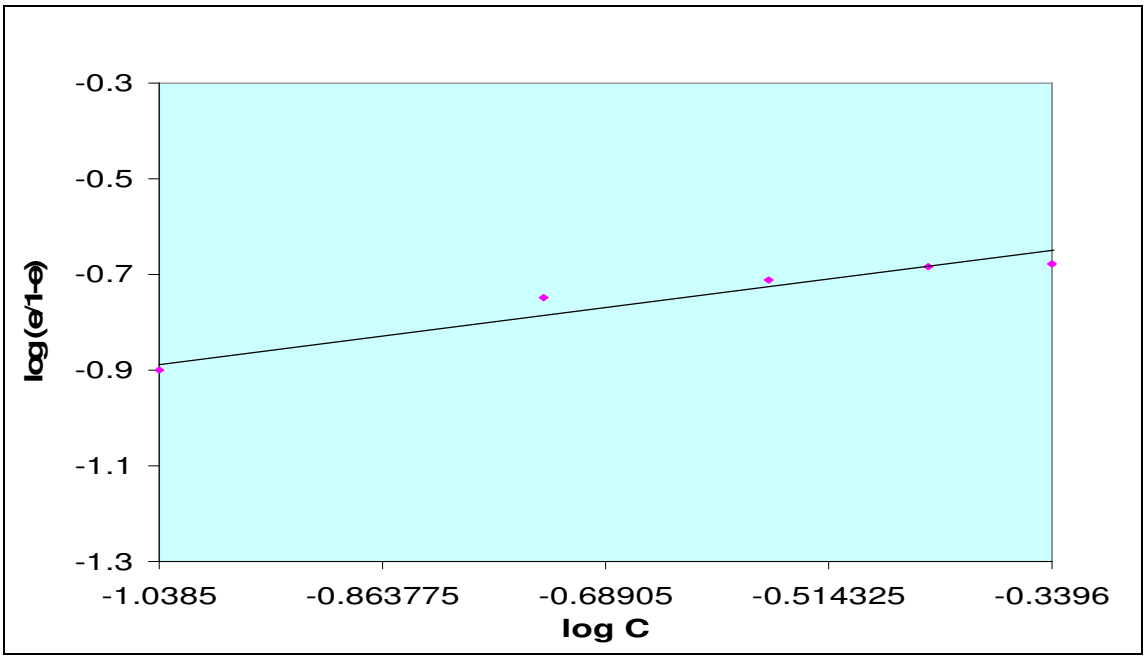

Fig.-7: Thermodynamic Kinetic Model for AA1100 at 72 h and 30 ± 1 ^{0}C.

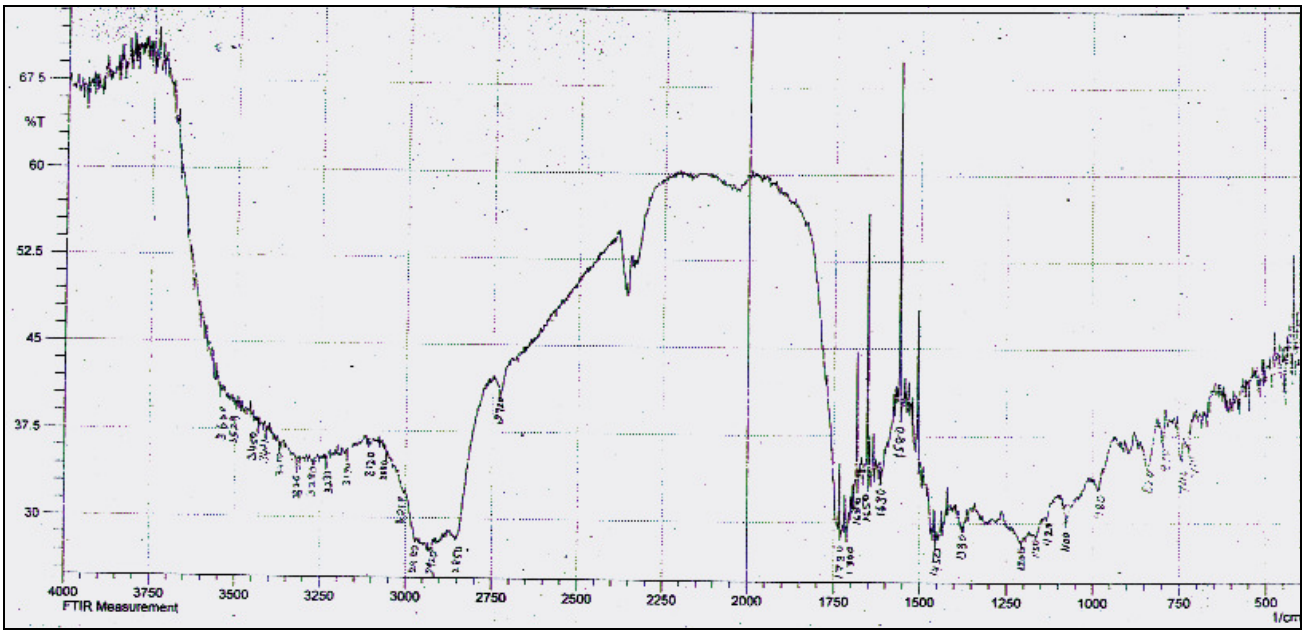

Fig.-8: FT-IR spectra of EE*PnLS*.

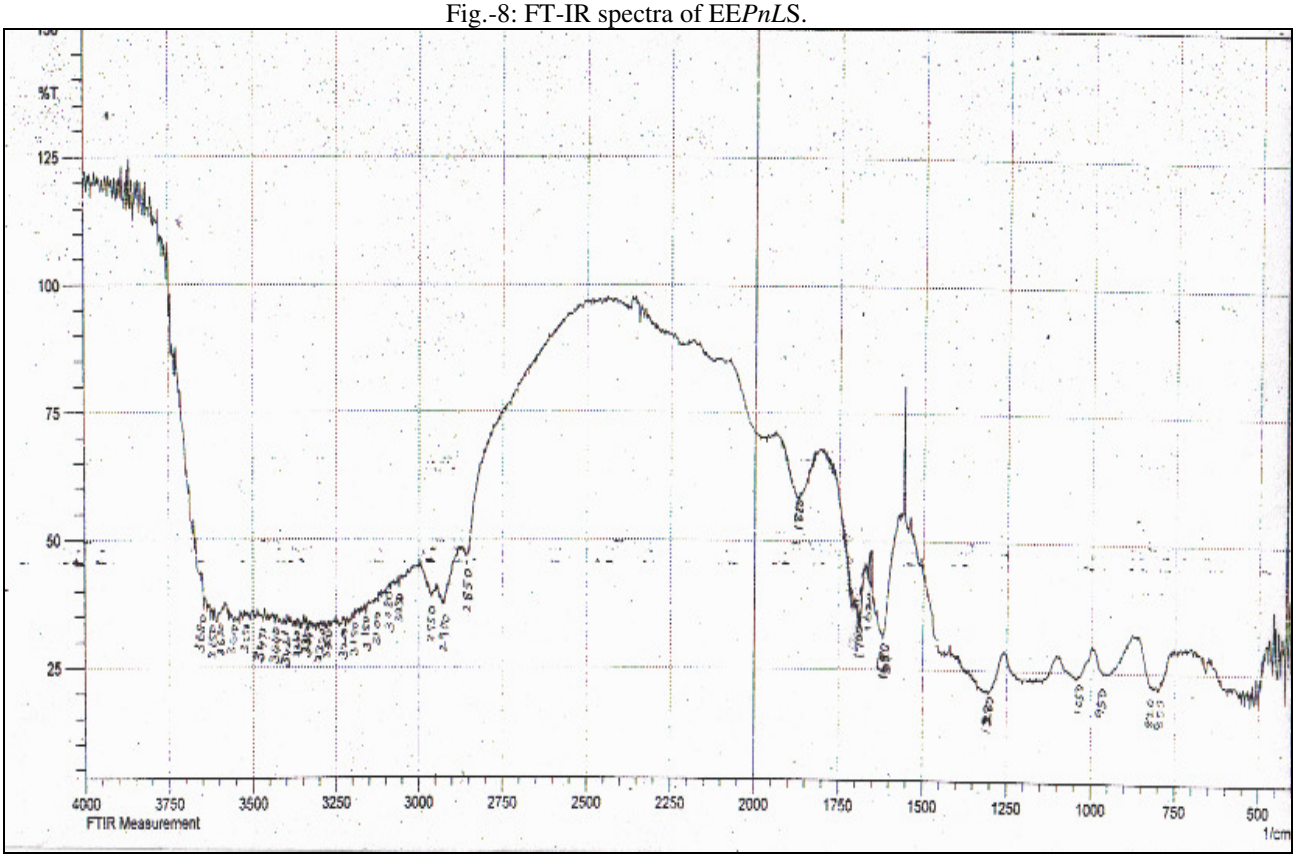

Fig.-9: FTIR spectra of adsorbed film of EE*PnLS* over AA1100 immersed in 0.5 M HCl containing 0.4575 g/L EE*PnLS*.

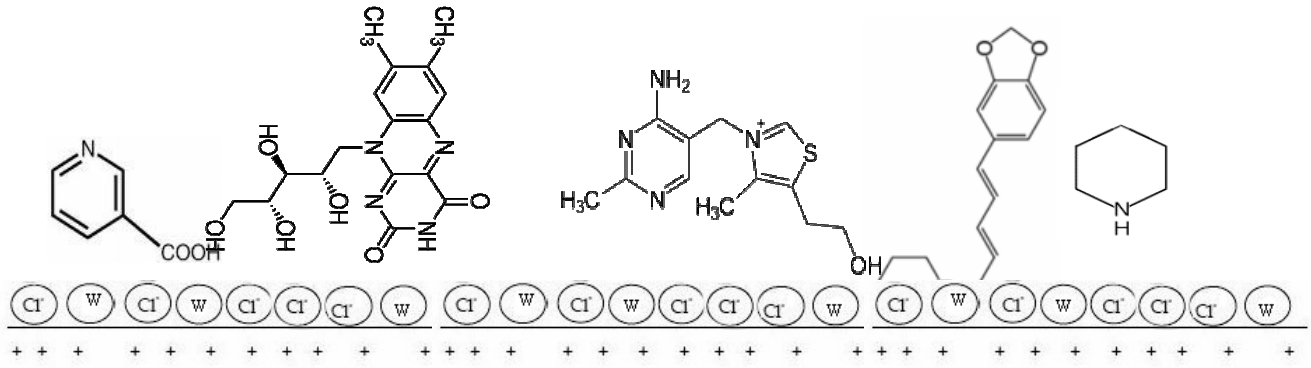

Fig.-10: A sketch representing one of the possible orientations of the active organic constituents of EE*PnLS* during the adsorption phenomenon over AA1100 surface.

Table-1: Corrosion Parameters of Acid Corrosion of AA 1100 without and with different Concentrations (g/L) of EE*PnLS* at various Immersion Time (h) at temperature 30 ± 1 ^{0}C in 0.5 M HCl.

Time (h)	EE*PnLS* Concentration (g/L)	Corrosion Parameters				
		Weight loss (mg)	Corrosion Rate (ρ_{corr}) (mmy^{-1})	Inhibition Efficiency (IE %)	Fractional Surface Coverage (θ)	Adsorption Equilibrium Constant (K_{ad}) (mol/L)
72	S-0 0.0000	102.7	3.43	--	--	--
	S-1 0.0915	58.6	1.96	42.94	0.43	8.22
	S-2 0.1830	56.2	1.88	45.28	0.46	4.57
	S-3 0.2745	35.9	1.20	65.04	0.65	6.78
	S-4 0.3660	22.5	0.75	78.09	0.78	9.74
	S-5 0.4575	14.7	0.49	85.69	0.86	13.08
144	S-0 0.0000	157.5	2.63	--	--	--
	S-1 0.0915	122.5	2.04	22.22	0.22	3.12
	S-2 0.1830	107.5	1.79	31.75	0.32	2.54
	S-3 0.2745	89.9	1.50	42.92	0.43	2.74
	S-4 0.3660	83.0	1.39	47.30	0.47	2.45
	S-5 0.4575	59.2	0.99	62.41	0.62	3.63
216	S-0 0.0000	164.0	1.83	--	--	--
	S-1 0.0915	148.6	1.65	9.39	0.10	1.13
	S-2 0.1830	135.3	1.50	17.50	0.18	1.16
	S-3 0.2745	117.2	1.30	28.54	0.28	1.45
	S-4 0.3660	113.3	1.26	30.91	0.31	1.22
	S-5 0.4575	99.7	1.11	35.26	0.35	1.18
288	S-0 0.0000	177.5	1.48	---	---	---
	S-1 0.0915	161.2	1.35	9.18	0.09	1.10
	S-2 0.1830	150.6	1.26	15.15	0.15	0.98
	S-3 0.2745	148.6	1.24	16.28	0.16	0.71
	S-4 0.3660	147.1	1.23	17.17	0.17	0.57
	S-5 0.4575	146.7	1.22	17.35	0.17	0.46